



IN-DUCT BROADBAND DISSIPATION USING MICRO-CAPILLARY PLATES

Teresa Bravo María^{1}*
Cédric Maury²

¹Instituto de Tecnologías Físicas y de la Información “Leonardo Torres Quevedo” (ITEFI), Consejo Superior de Investigaciones Científicas (CSIC), Madrid, Spain

²Ecole Centrale Marseille, Laboratory of Mechanics and Acoustics (LMA), Marseille, France

* *Autor de contacto:* teresa.bravo@csic.es

Copyright: ©2023 Bravo et al. This is an open-access article distributed under the terms of the Creative Commons Attribution 3.0 Unported License, which permits unrestricted use, distribution, and reproduction in any medium, provided the original author and source are credited.

ABSTRACT

Attenuation of low frequency noise constitutes a long-standing problem in the field of noise control. The use of Micro-Perforated Panels has been proved to be efficient if the primary noise source spectrum is confined in a narrow frequency band. To get rid of the limitations due to the backing cavity depth, unbacked configurations have also been considered. They are able to supply good attenuation results if the size of the hole diameters is reduced and the perforation ratio is increased. These devices are denoted Micro-Capillary Plates. These ultra-perforated membranes consist of highly porous panels made up of leaded glass, of high porosity with millions of micro-channels per centimeter square, the holes or square channel dimensions varying between $5\mu\text{m}$ and $50\mu\text{m}$. They are 1-2 millimeters thick and can be produced in various shapes using drawn tubes of fused, chemically etched fibers, working on both backed or unbacked configurations. These characteristics provide them with exceptional acoustical properties compared to other classical absorbers or MPPs. If rigidly backed by an air cavity of 24 mm, a MCP device provides a half-bandwidth absorption over 12 octaves whereas a MPP device works only over one-two octaves. Their performance will be examined in ducted propagation conditions.

Key-words— Broadband absorption, micro-capillary plates, low-frequency noise control.

1. INTRODUCTION

The problem of noise control has traditionally posed a tremendous threat to human health and living quality [1]. As typical dimension of a structure is of the order of the wavelength of the sound, for low frequency sound, conventional methods are impractical because they result in structures too bulky to handle. Traditional noise control materials present inherent weak absorption and transmission performance in the low frequency due to the limited viscous and thermal frictional dissipation between air and solid interfaces [2]. Sound absorbers need generally to be protected from the surrounding environment, by covering them with an impervious membrane, such as a plastic sheet or a layer of paint, that significantly decreases the absorption at high frequencies, which is usually highly undesirable [3]. A common solution is to use a perforated facing as a covering for the classical porous materials, which also changes the absorption characteristics. They are characterized by their flow resistivity which is a function of their perforation rate or porosity, their perforation size or flow resistivity and their perforation thickness.

Since the 1980s, a series of applications in demanding environments claimed for more effective non-fibrous absorptive materials. These included especial hygienic and cleaning conditions, high temperature, high-speed flow and

humidity. Maa [4, 5] developed the theory for Micro-Perforated Panels (MPPs), with perforations of sub-millimeters in diameter or slits in width, and they have been widely used in architectural acoustics and noise control engineering design. Applications include any place where non-fibrous sound absorptive materials are expected such as in air-flow duct [6, 7]. They can be manufactured from different materials such as cardboard, plastic or plywood, constituting an ecological and recyclable option for light and soundproof solutions. One important characteristic of MPPs is that they can be designed according to specific absorption characteristics by the proper optimization of the physical constitutive parameters, that makes them flexibly tuned absorbers.

However, despite all these applications and advantages, MPPs can be considered as Helmholtz Resonators with important attenuation values but confined in a narrow frequency band. Band absorption for typical MPP parameters cannot exceed two octaves. Several solutions have been proposed to enhance the control frequency domain, being the use of multi-layer configurations [8]. The optimal layout sequences are found by computing the resonance frequencies of the resulting acoustic system, improving the sound absorption bandwidth but at the expense of increasing of the total thickness of the sound absorber [9]. Another similar approach is to use arrangements of multiple MPPs with a multi-depth cavity with partitioned sections. It has been concluded that by increasing the number of partitions in the cavity, a wide uniform range of absorption can be attained but maxima of absorption would be dropped [10], presenting a trade-off between maximum absorption coefficient and wide-band performance.

To avoid limitations associated to the resonant frequencies of the combined MPPs arrays, some authors [11] have started to consider unbacked absorbers that can be used in aeronautics applications, where cavity space is reduced at maximum. Numerical simulations have shown that unbacked micro-perforated membranes with holes diameters down to $10\mu\text{m}$ can provide wideband absorbing and insulating devices in the low frequency range when increasing the perforation ratio [12]. However, there has been a lack of convenient and affordable method to build freestanding perforated membranes within the required specifications. Recently, they have been made of solid polymer and with holes diameters down to $10\mu\text{m}$ using photolithography [13]. Such ultra micro-perforated membranes, denoted as Micro-Capillary-Plates (MCPs), are used in bio-MEMS applications to pattern surfaces in various materials and to fabricate three-dimensional channel structures. Although current applications include their use as image intensifiers or as detectors of cosmic rays in particle physics, their properties in the field of acoustics for efficient dissipation in the low frequency range have not been studied yet. It has been suggested that they appear to be potentially

good candidates for the design of wideband sound absorbing and insulating MPPs that could meet the highly resistive impedance boundary conditions [11].

In this work, we will study the absorption, transmission and dissipative properties of MCPs for different configurations of their constitutive parameters. Predictions by analytical formulations and experimental verification of the expected results will confirm the validity of MCPs as broadband absorbers in the low frequency range. Section 2 will describe the characteristics of the MCPs samples analysed in this work, with a wide range of design parameters. Section 3 will proceed with a theory comprising two different regimens of interest for the MCPs, the continuous model and the slip-flow model. Using the slip-flow regimen, a parametric study is presented for the prediction of the acoustical dissipation properties that may be expected, for different MCP configurations. These results are confirmed in Section 4 against an experimental study carried out in a laboratory environment with different MCP load conditions. The work finishes with a summary of the main conclusions and some ideas for future research.

2. DESCRIPTION OF THE MCP SAMPLES

MCPs are structures built on a highly resistive material that are composed of many identical parallel cylindrical channels distributed uniformly over the surface. In contrast with traditional MPP devices, MCPs have micro-holes with diameter typically lower than $50 \mu\text{m}$ and a perforation ratio greater than 50 %. The typical thicknesses are similar for all configurations, varying between 1 mm to several mms. Figure 1 presents the glass capillary array that has been used in this work.

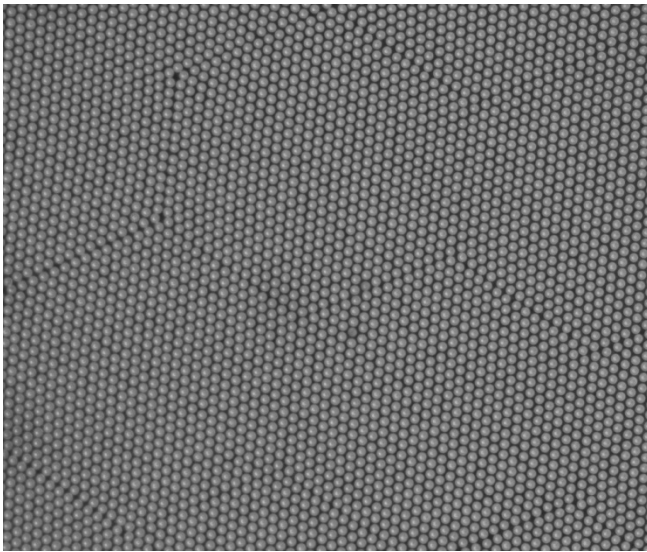


Figure 1. Photograph of the MCP sample when magnified by an electronic microscope.

The augmented image has been acquired with an electronic microscope. The characteristic parameters include the holes diameter, d , the holes pitch Λ and the panel thickness t . In case the MCP is used in a cavity-backed configuration, the thickness of the backing cavity, denoted by D , has also to be considered.

From Figure 1 we can distinguish the hexagonal-staggered hole distribution with a 60° staggering angle. The classical perforation ratio for a classical square mesh distribution computed as $\sigma = \pi d^2 / (4\Lambda^2)$ has to be recalculated for this configuration as $\sigma = \pi d^2 / (2\sqrt{3}\Lambda^2)$.

Next sections will study acoustic performance of two different MCPs compared to those of classical MPPs. The physical characteristics of the four different panel types are presented in Table 1.

Table 1. Physical parameters for two MCPs samples used in this work and those for two MPPs.

Sample type	Channel radius [μm]	Channel pitch [μm]	Perforation Ratio [%]	Thickness [mm]
MCP 1	15	32	79.71	1
MCP 2	12.5	33.5	50	0.5
MPP 1	440	2500	9.73	1
MPP 2	440	3000	6.76	1

3. ANALYTICAL FORMULATION

3.1. Slip-flow regimes

The formulation of an appropriate analytical model for acoustic characterisation of MCPs samples is presented in this section. Well-established continuous laws that have been used for analysis of microperforated partitions may not hold in this new configuration. Rarefaction effects should be considered in the field of microfluidics when characteristic lengths are of the order of $1 \mu\text{m}$ [14], as in the case of MCPs micro-channels.

A regime classification can be done in terms of the ratio between the molecular mean free path, λ , and the characteristic length L of the control volume, that is taken for MCPs as the diameter of the perforations. This quantity is called the Knudsen number and takes the expression,

$$\text{Kn} = \lambda / L . \quad (1)$$

It characterizes rarefaction effects within the micro-channels [15]. The condition $\text{Kn} \ll 1$ constitutes the requirement for thermodynamic equilibrium. In particular,

when $Kn < 10^{-3}$, the flow is in the continuum regime and classical continuity boundary conditions at the channel walls are fulfilled. On the other hand, when $10^{-3} \leq Kn \leq 10^{-1}$, the flow is in the slip-flow regime. In this regime, a velocity slip and a temperature jump are observed at the boundary wall, affecting the fluid flow and the heat transfer. When the fluid is moving in the direction parallel to the wall-fluid interface, a slip velocity $v_{slip} = v_{\Sigma}$ appears defined as the difference between the axial particle velocity, v , and the velocity at the pore wall surface v_{wall} , as indicated in Fig. 2. Typically, most of the microsystems that work with gases are in the slip flow regime.

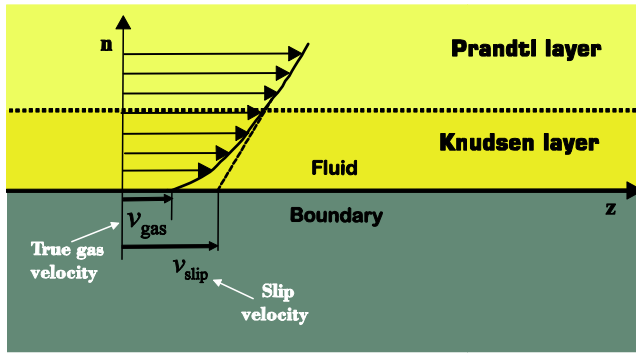


Figure 2. Knudsen layer and slip-flow regime for the MCP modelization.

Using a first-order Taylor expansion to express the equilibrium of momentum at the wall Σ , the slip velocity can be expressed as

$$v_{\Sigma} = \frac{2 - \sigma_v}{\sigma_v} Kn \left. \frac{\partial v}{\partial n} \right|_{\Sigma} \quad (2)$$

where σ_v is a coefficient that can be calculated from the kinetic theory of gases [16] impinging on the surface considering that for every unit of area, a fraction σ_v of the molecules is absorbed by the surface.

Assuming straight cylindrical channels in harmonic regime ($e^{j\omega t}$), linearized momentum and energy conservation lead to the viscous transfer impedance of a micro-channel, given per unit length by

$$Z_v = j\omega\rho_0 t \left\{ 1 - \frac{2}{k_v r_0} \frac{J_1(k_v r_0)}{[J_0(k_v r_0) - B_v k_v r_0 J_1(k_v r_0)]} \right\}^{-1} \quad (3)$$

where $k_v = \sqrt{-j\omega\rho_0/\mu}$ is the viscous diffusion wavenumber, μ the air dynamic viscosity, ρ_0 the air

density, and J_0 and J_1 are the Bessel functions of the first kind of orders 0 and 1 respectively. From Eq. (3), one can simulate the acoustic performances of MCP samples in slip-flow regime. Assuming plane wave normal incidence, the amplitude reflection and transmission coefficients are defined as $r = (Z_1 - Z_0)/(Z_1 + Z_0)$ and $\tau = 2Z_0/(Z_1 + Z_0)$ with $Z_1 = Z_v/\sigma + Z_0$, the input impedance of the absorber backed by an anechoic termination, and $Z_0 = \rho_0 c_0$. One can then calculate the dissipation, $\eta = 1 - |r|^2 - |t|^2$, as the fraction of incident energy not reflected, nor transmitted. It is expressed as a function of $\alpha = 1 - |r|^2$ (resp. $t = |t|^2$) the energetic absorption (resp. transmission) coefficients.

3.2. Parametric study

A parametric study has been carried out considering the equations implemented in the previous section for the evaluation of the performance of the proposed MCPs. The acoustic performance of both an unbacked MCP and an unbacked MPP have been compared in Figure 3 as a function of frequency showing the dissipation values and the real and imaginary parts of the specific transfer impedance.

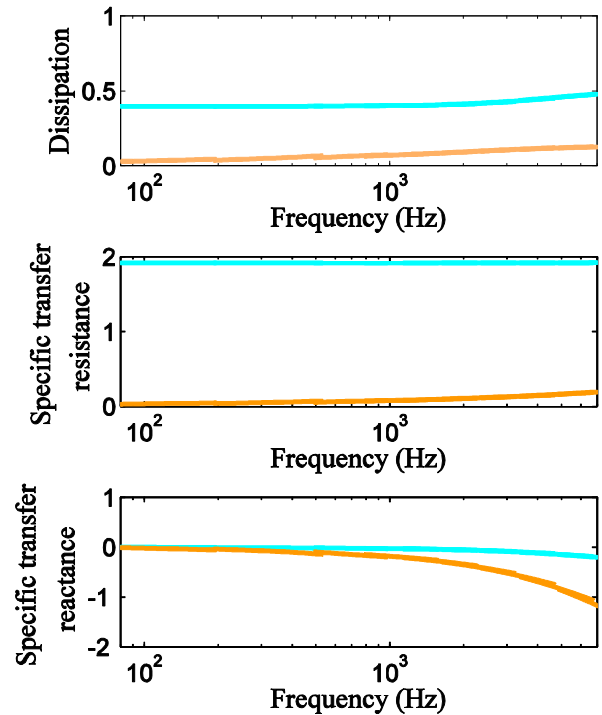


Figure 3. Normal incidence dissipation (top) and their corresponding specific input resistance (middle) and reactance (bottom) for the unbacked MCP1 (blue) and MPP1 (orange).

It can be appreciated that the dissipation values remain low for the MPP sample, whereas when the physical parameters of the MCP have been selected appropriately, the optimal dissipation value of 0.5 is achieved that extends over the whole low frequency range up to 10 kHz.

This trend can be better understood when observing the corresponding real and imaginary parts of the specific input impedance. The MPP presents a specific resistance that approaches zero in the low frequency range, but progressively increases as frequency gets higher. This is not the case for the MCP that shows a specific resistance almost constant over a broader low-frequency range. It can be stated then that the MCP acts as a pure resistance layer, with a real part that can be adjusted by a proper selection of the physical parameters and an imaginary part that remains zero over a broad band in the low frequency range.

4. EXPERIMENTAL VALIDATION

4.1. Experimental set-up

The validation of the predicted results has been carried out in a controlled semi-anechoic chamber. The acoustic performance of different samples has been estimated using a small Kundt tube, as it can be seen in Figure 4. The upper frequency is calculated considering the inner radius of the tube, $R = 1.5 \text{ cm}$, that determines the cut-off frequency of the plane wave modes and provides a maximum frequency of analysis slightly less than 6700 Hz.

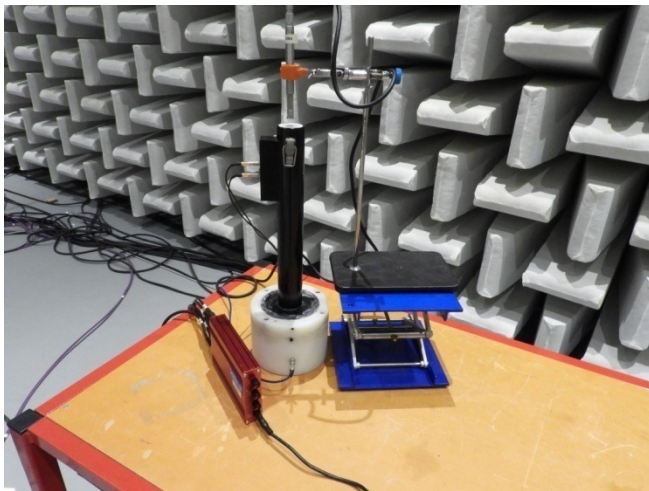


Figure 4. Photograph of the experimental set-up situated in a semi-anechoic chamber, composed of a small Kundt tube connected on one side to a loudspeaker and closed by the MCP sample.

The base of the Kundt tube is connected to a loudspeaker driven to produce a white noise between 80 Hz and 6.7 kHz, with a sampling rate of 12.8 kHz and a spectral resolution of 1.56 Hz. This noise propagates downstream the small Kundt

tube to the termination where the MCP sample is inserted, as it can be seen in Figure 5.



Figure 5. Detail of the sample holder that supports the MCP radiating in free-field conditions.

It can be appreciated that the surface occupied by the MCP sample is smaller than the cross-section area of the Kundt tube. A thick PVC adaptor was printed that provides an optimal connection between the duct and the sample.

The acquisition procedure is driven by the OROS multichannel system that generates one output to the loudspeaker amplifier and takes the inputs of the microphones situated along the duct length. We have used the two-microphone method for the determination of the sample absorption coefficient [17]. Two 1/4" condenser microphones has been situated with a separation distance between them equal to $d = 5 \text{ cm}$, providing a lower cut-on frequency of analysis equal to 200 Hz for this configuration.

A measurement of the near-field pressure and acoustic particle velocity have also been acquired simultaneously using a miniature pressure-velocity probe [18] located in the proximity of the radiating side. This allows the calculation of the load radiation impedance behind the MCP, that presents an important influence on the acoustical performance outcomes.

4.2. Dissipation performance

The predicted results will be compared with the experimental characterization in this section for the MCP1, with the physical parameters presented in Table 1. It should be noted that the predictions when considering anechoic radiation loads are underestimated in the low frequency range. To obtain a reasonable agreement, we need to take into account the load radiation impedance for the sample holder that has been predicted analytically considering the model of Silva *et al.* [19]. These results are presented with the dotted-green line in Figure 6. The same quantity has also

been estimated using the near-pressure and acoustic velocity measurements acquired with the pressure-velocity probe (solid green line). The absorption coefficients measured and estimated for the free-standing MCP sample are superimposed in Figure 6 represented in blue (solid and dotted respectively).

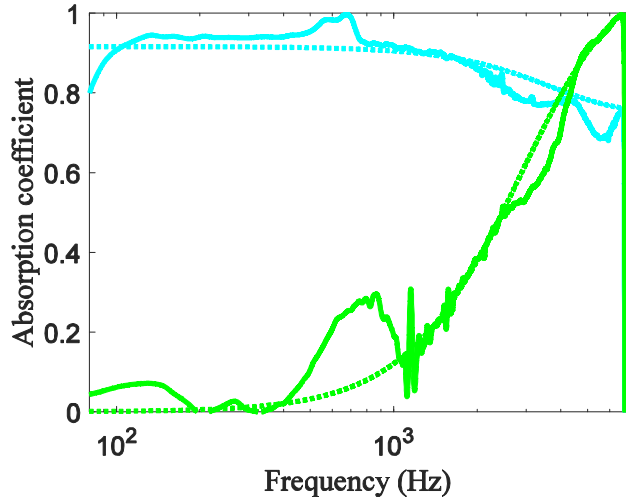


Figure 6. Normal incidence absorption coefficient for the unbacked MCP1: measured values (solid blue) and estimated analytically (dotted blue); the measured (solid green) and the predicted (dotted green) absorption of the open adaptor termination is also shown.

It can be seen that when including this correction for the radiation impedance of the MCP unbacked sample, the agreement of predictions and measurements for the absorption coefficient is good over the frequency range of analysis. We can state that the MCP achieves constant values of absorption of around 0.9 up to 1 kHz that then slowly decrease when increasing the frequency.

4.3. Comparison with classical materials

To evaluate the extent of the obtained outcomes for the proposed devices, in this section we will perform a comparison with other classical samples. To point out the influence of the physical constitutive parameters, we will first make a comparison between the MCP1 that has been analyzed in the previous section, and the MCP2 that presents a panel thickness half of the corresponding for the MCP1 (0.5 mm), and a smaller value of the perforation ratio (50%). The comparison between the predictions (dotted lines) and the measurements (solid lines) for both MCPs are presented in blue in Figure 7.

It can be appreciated that the performance of both samples is quite good in the low-frequency band, but the differences introduced on the thickness and the separation distance between holes provide an absorption coefficient that differs mostly on the behavior as a function of the

frequency. The value provided when considering an average absorption coefficient is higher for the MCP1 (light blue) that for the MCP2 (dark blue), with a similar broadband and flat performance on the low frequency range. However, it can be appreciated that the MCP2 is able to provide superior values in the very low frequency range that overtake those obtained with the MCP1. This outlines the important differences that can be obtained in the absorption performance when varying one or several parameters. In this sense, we could say that the MCP proposed in this work can be considered as acoustic metamaterials as they can be adjustable subwavelength devices that can be tuned to the required noise control objectives for each particular problem by the selection of the constitutive parameters.

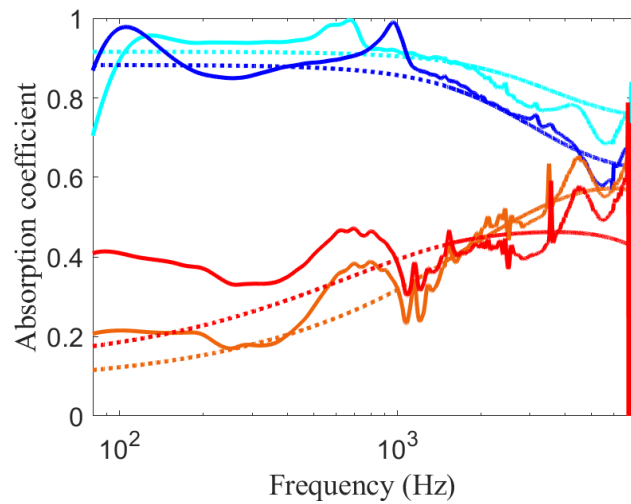


Figure 7. Normal incidence absorption coefficient for the measured (solid) and estimated analytical values (dotted) for the two unbacked MCP1 (light blue) and MCP2 (dark blue) compared to the classical MPP1 (red) and MPP2 (orange).

A comparison with other classical materials is also presented in Figure 7. In particular, we have included the absorption coefficients for two classical MPPs, with the physical characteristics outlined in Table 1. They both present a thickness of 1 mm, the same channel radius (0.44 mm) and slightly different values of the holes separation distance that provides similar perforation ratios that stays below the 10%. Although these are typical MPP parameters it should be noted that they have not been optimized for any particular purpose.

The measured absorption coefficients for MPP1 (red solid line) and MPP2 (orange solid line) have been measured in exactly the same conditions using the small Kundt tube situated in the semi-anechoic chamber. They results are presented in Figure 7 and superimposed to the analytical prediction using Maas model. As expected, the obtained performance is well-below those obtained with the MCP samples, although they maintain an almost-constant value below 1 kHz, with average absorption performance of

around 0.4 for MPP1 and 0.25 for MPP2. It should be kept in mind that the samples are working in unbacked, free-standing conditions. This explains the differences with the cavity-backed configurations where an absorption coefficient close to unity can be easily achieved at the Helmholtz resonance of the backing cavity. This outlines the importance of the proposed MCP materials as they allow to get rid of the backing cavity, that imposes heavy limitations in terms of dimensions, and maintaining optimal and broadband values in the low frequency range.

5. CONCLUSIONS

As an alternative to classical porous or fibrous materials for broadband and low-frequency noise control, this work proposes the possibilities of micro-capillary plates to act as wideband absorbers in this frequency range. The main characteristics of these devices are the dimensions of the hole diameters, of the order of the micrometers, and the high perforation ratio or porosity, overtaking the 50% for good performance.

Under these conditions, well-established continuum laws may not hold and alternative descriptions should be formulated for a prediction of the acoustic behavior of the MCPs. Due to Knudsen number values, transfer impedances for MCPs have been derived in the frame of the slip-flow regime that significantly deviates from the classical approach for very small channel radius, when characteristic lengths are of the order of 1 μm . Parametric studies have shown that due to their micrometric channels radius and high porosity, MCPs are pure resistive absorbers with constant resistance and minute reactance over a wide frequency band.

A set of experiments performed in a semi-anechoic chamber have validated that unbacked optimal MCPs can achieve absorption values greater than 0.9 up to 4 kHz under normal incidence. They constitute an alternative to other classical devices, such as MPPs, without limitations on the backing cavity size. Further research work could be directed towards the study of the acoustic performance to other plane waves incident angles and to different excitation pressure fields.

9. ACKNOWLEDGMENTS

This work is part of the project TED2021-130103B-I00, funded by MCIN/AEI/10.13039/501100011033 and the European Union "NextGenerationEU"/PRTR. It has also received support from the French government under the France 2030 investment plan, as part of the Initiative d'Excellence Aix-Marseille Université - A*MIDEX (AMX-19-IET-010).

12. REFERENCES

- [1] U. Ingard, *Noise Reduction Analysis*, Jones and Bartlett Publishers, Sudbury, Massachusetts, 2010.
- [2] C. Zwikker and C. W. Kosten, *Sound Absorbing Materials*, Amsterdam, Elsevier Press, 1949.
- [3] T.J. Cox and P.D'Antonio, *Acoustic absorbers and diffusers – Theory, Design and Application*, Spon Press, London, 2004.
- [4] D. Y. Maa, "Potential of microperforated panel absorbers," *Journal of the Acoustical Society of America*, vol. 104, pp. 2861–2866, 1998.
- [5] D. Y. Maa, "Microperforated-panel wideband absorbers," *Noise Control Engineering Journal*, vol. 29, pp. 77–84, 1987.
- [6] Y. Guo, S. Allam and M. Åbom, "Micro-perforated Plates for Vehicle Application", in *Proceedings of Internoise 2008*, (Shanghai, China), pp. 1918–1936, 2008.
- [7] S. Allam and M. Åbom, "A New Type of Muffler Based on Microperforated Tubes", *ASME Journal of Vibration and Acoustics*, vol. 133, pp. 1–8, 2011.
- [8] T. Bravo, C. Maury and C. Pinhède, "Enhancing sound absorption and transmission through flexible multi-layer micro-perforated structures", *Journal of the Acoustical Society of America*, vol. 134, no. 5, pp. 3663–3673, 2013.
- [9] N. N. Kim and J. S. Bolton, "Optimization of multi-layer microperforated systems for absorption and transmission loss", in *Proceedings of NoiseCon'14*, Advancing the Technology and Practice of Noise Control Engineering, (Florida, United States), pp. 8-10, 2014.
- [10] C. Wang and L.H. Huang, "On the acoustic properties of parallel arrangement of multiple micro-perforated panel absorbers with different cavity depths", *Journal of the Acoustical Society of America*, vol. 130, no. 1, 2011.
- [11] C. Maury and T. Bravo, "Wideband sound absorption and transmission through micro-capillary plates: Modelling and experimental validation", *Journal of Sound and Vibration*, vol. 478, pp. 115356, 2020.
- [12] T. Bravo and C. Maury, "Assessing the broadband absorption properties of micro-capillary plates through modelling and experimental studies", *POMA*, vol. 42, pp. 040002, 2021.
- [13] Y. Zheng, W. Dai, D. Ryan and H. Wu, "Fabrication of freestanding, microperforated membranes and their applications in microfluidics," *Biomicrofluidics*, vol. 4, pp. 036504, 2010.
- [14] S. Kandlikar, S. Garimella, D. Li, S. Colin and M. R. King, *Heat Transfer and Fluid Flow in Minichannels and Microchannels*, Elsevier Ltd., Oxford, 2nd Edition, 2014.
- [15] V. F. Kozlov, A. V. Fedorov, N. D. Malmuth, Acoustic properties of rarefied gases inside pores of simple geometries, *J. Acoust. Soc. Am.* 117, 3402–3412, 2005.
- [16] J. C. Maxwell, On Stresses in Rarefied Gases Arising from Inequalities of Temperature, *Phil. Trans. Roy. Soc. Part I* 170, 1879.
- [17] ASTM E1050-12, Standard Test Method for Impedance and Absorption of Acoustical Materials Using a Tube, Two Microphones and a Digital Frequency Analysis System, ASTM International, West Conshohocken, U.S.A., 2012.
- [18] T. Bravo and C. Maury, "Sound attenuation and absorption by anisotropic fibrous materials: Theoretical and experimental study", *Journal of Sound and Vibration*, vol. 417, pp.165–181, 2018.
- [19] F. Silva, Ph. Guillemain, J. Kergomard, B. Mallaroni, A. Norris, "Approximation formulae for the acoustic radiation impedance of a cylindrical pipe", *Journal of Sound and Vibration*, vol. 322, pp. 255–263, 2009.